Food and Chemical Toxicology 123 (2019) 536–545

Contents lists available at ScienceDirect

Food and Chemical Toxicology

journal homepage: www.elsevier.com/locate/foodchemtox

Pterostilbene protects against acetaminophen-induced liver injury by restoring impaired autophagic flux

Ki-Young Kang[1], Jun-Kyu Shin[1], Sun-Mee Lee[*]

School of Pharmacy, Sungkyunkwan University, Suwon, 440-746, Republic of Korea

ARTICLE INFO

Keywords:
Pterostilbene
Acetaminophen
Oxidative stress
Hepatotoxicity
Autophagic flux

ABSTRACT

An overdose of acetaminophen (APAP) causes liver injury through formation of *N*-acetyl-*p*-benzoquinoneimine, which overproduces reactive oxygen species (ROS). Autophagy maintains cellular homeostasis and is regulated by generation of ROS. Pterostilbene (PTE) has been shown to have antioxidant and anti-inflammatory properties. In this study, we investigated the protective mechanisms of PTE against APAP-induced liver injury, focusing on autophagy. ICR mice were intraperitoneally (i.p.) treated with 400 mg/kg of APAP. PTE (15, 30, and 60 mg/kg, i.p.) and chloroquine (CQ, 60 mg/kg, i.p.) were injected 1 h after APAP treatment. Blood and liver tissues were isolated 6 h after APAP treatment. PTE decreased serum aminotransferase activities and hepatic oxidative stress; this protective effect was abolished by CQ. APAP impaired autophagic flux, as evidenced by increased microtubule-associated protein-1 light chain 3-II and p62 protein expression; this impaired autophagic flux was restored by PTE, while CQ abolished this effect. APAP decreased beclin-1 and autophagy related protein 7 protein expressions, while PTE attenuated these decreases. PTE increased the lysosome-associated membrane protein-2 protein expression and decreased the mammalian target of rapamycin and Unc-51 like autophagy activating kinase 1 phosphorylation. Our findings suggest that PTE protects against APAP-induced hepatotoxicity by enhancing autophagic flux.

1. Introduction

Acetaminophen (APAP) is widely used as an antipyretic and analgesic agent with a very high safety profile when used properly. If misused, either intentionally or accidentally, acetaminophen can cause significant liver injury (Larson, 2007; Amar and Schiff, 2007). Excessive production of reactive oxygen species (ROS) is the main pathogenesis of APAP overdose, which is mediated by *N*-acetyl-*p*-benzoquinone imine, a metabolite of APAP (James et al., 2003). The resulting oxidative stress triggers mitochondrial dysfunction, membrane permeability transition, and DNA fragmentation, leading to impaired cellular homeostasis and cell death (Jaeschke et al., 2012). *N*-Acetylcysteine (NAC), a representative antioxidant agent, is a therapeutic option for APAP-induced hepatotoxicity in humans (Lee et al., 2009). However, it was reported that NAC overdose in the treatment of APAP-induced hepatotoxicity has side effects such as acute renal failure, hemolysis, and thrombocytopenia, which finally lead to death (Mahmoudi et al., 2015). In addition to NAC, natural foods or food-derived substances such as silymarin, curcumin, and reseveratrol (RSV) are known to relieve APAP-induced liver failure (Park et al., 2013; Muriel et al., 1992; Sener et al., 2006; Somanawat et al., 2013; Jaeschke et al., 2011).

Autophagy, a self-digestion system involving degradation of dysfunctional or damaged components, is a dynamic process by which autophagic substrates are sequestered in autophagosome and degraded on fusion with lysosomal components, i.e. the autolysosome. The updated consensus suggests that real status of autophagy should be assessed not only by the number of autophagosomes and autolysosomes but also by evaluating the actual autophagic flux, such as monitoring the clearance of cell components in autolysosomes (du Toit et al., 2018). Recent studies have uncovered the critical linkage between

Abbreviations: ALT, alanine aminotransferase; AMPK, 5′ adenosine monophosphate-activated kinase; APAP, acetaminophen; AST, aspartate aminotransferase; Atg, autophagy-related protein; CQ, chloroquine; GSH, glutathione; GSSG, oxidized glutathione; H&E, hematoxylin and eosin; LAMP, lysosomal associated membrane protein; LC3, microtubule-associated protein-1 light chain 3; MDA, malondialdehyde; mTOR, mammalian target of rapamycin; NS, normal saline; PTE, pterostilbene; p62, sequestosome1/p62; ROS, reactive oxygen species; SEM, standard error of the mean; TBS/T, 0.1% Tween 20 in 1× Tris-buffered saline; TEM, transmission electron microscopy; ULK1, Unc-51 like autophagy activating kinase 1

[*] Corresponding author. School of Pharmacy, Sungkyunkwan University, Seobu-ro 2066, Jangan-gu, Suwon, Gyeonggi-do, 440-746, Republic of Korea.
E-mail addresses: allzzangjk@naver.com (J.-K. Shin), sunmee@skku.edu (S.-M. Lee).

[1] These authors equally contributed to this work.

https://doi.org/10.1016/j.fct.2018.12.012
Received 31 August 2018; Received in revised form 7 December 2018; Accepted 8 December 2018
Available online 10 December 2018
0278-6915/

oxidative stress and autophagy in human disease. In heart ischemia/reperfusion (I/R), excessive ROS impaired autophagy and autophagy restoration via rapamycin attenuated heart injury (Wu et al., 2014). In primary hepatocyte and the *in vivo* mouse liver, APAP treatment induced ROS accumulation and activated autophagy (Ni et al., 2012; Zai et al., 2018) In contrast, Wang et al. (2016) demonstrated that APAP overdose activates the ROS-TRPM2-Ca^{2+}-CAMK2-BECN1 cascade to inhibit autophagy, which is partially responsible for the induced liver damage. Adiponectin alleviated APAP-induced mitochondrial dysfunction by autophagy activation (Lin et al., 2014b). Although autophagy is involved in APAP-induced hepatotoxicity, the precise mechanism by which APAP overdose affects autophagic flux remains unclear.

Resveratrol (RSV) is a well-known member of the stilbenes and is found in grapes and other foods, which have antioxidant and anti-inflammatory properties. Pterostilbene (trans 3,5-dimethoxy-4-hydroxystilbene; PTE), a dimethylated derivative of RSV, is extensively found in grape and blueberry which is superior as compared to RSV in terms of bioavailability and lengthened half-life (Szajdek and Borowska, 2008; Kapetanovic et al., 2011). PTE has been reported to have a variety of biological activities including antioxidative (Rimando et al., 2002), anti-inflammatory (Lv et al., 2015), and anti-cancer (Lin et al., 2014a) activities. In clinical trials, daily administration of PTE to humans resulted in inhibition of PGE_2 activity (Hougee et al., 2005). PTE has been shown the pharmacological activity in various liver diseases. PTE attenuated lipid peroxidation and recovered glutathione (GSH) depletion in liver fibrosis (Lee et al., 2013). PTE showed anti-peroxidative effects via nuclear factor (erythroid-derived 2)-like 2 (Nrf) signaling in diabetic mice liver (Bhakkiyalakshmi et al., 2016). In SAS and OECM-1 human oral cancer cell lines, PTE had anti-proliferative effects by activating autophagy via modulation of the Akt pathway (Ko et al., 2015). Furthermore, PTE treatment induced autophagy via activation of 5′ adenosine monophosphate-activated protein kinase (AMPK) and subsequently inhibited apoptosis of human vascular epithelial cells (Zhang et al., 2013). Although PTE is a well-known antioxidant, the relationship between APAP and PTE has not yet been studied.

In this study, we aimed to investigate the molecular mechanisms by which PTE protects against APAP-induced liver injury, with a particular focus on the autophagic flux and its signaling pathway.

2. Materials and methods

2.1. Animals

Male ICR mice weighing 20–22 g (4 weeks old) were obtained from Daehan Biolink Inc. (Eumsung, Korea) and were acclimatized to laboratory conditions at Sungkyunkwan University for 7 days. Mice were maintained in a room with controlled temperature and humidity (25 ± 1 °C and 55 ± 5%, respectively) with a 12 h light-dark cycle, and water and food provided *ad libitum*. All animals received care in compliance with the Principles of Laboratory Animal Care formulated by the National Institute of Health (NIH publication No.86–23, revised 1985) and the guidelines of Sungkyunkwan University.

2.2. Treatment of animals

Mice were fasted for 18 h before each experiment but were given tap water *ad libitum*. Except for controls, mice were intraperitoneally (i.p.) injected with APAP (400 mg/kg; Sigma-Aldrich, St Louis, MO, USA) dissolved in warm normal saline (NS). PTE (15, 30, and 60 mg/kg, i.p.; Tokyo Chemical Industry Co., LTD., Tokyo, Japan) and RSV (53 mg/kg, i.p.; Sigma-Aldrich) as a positive control were dissolved in 10% Tween 80/saline (vehicle) and administered 1 h after APAP treatment. Chloroquine (CQ; 60 mg/kg, i.p.), an autophagy inhibitor, was dissolved in NS and administered 1 h after APAP treatment. The dose and timing of APAP, PTE, and CQ administration were determined based on earlier reports and our preliminary studies (Cho et al., 2016; Lee et al., 1999; McCormack and McFadden, 2012). Animals were randomly divided into eleven groups as follows (n = 6–8): 1) vehicle-treated control group (Control + Vehicle), 2) 60 mg/kg PTE-treated control group (Control + PTE60), 3) 53 mg/kg RSV-treated control group (Control + RSV53), 4) vehicle-treated APAP group (APAP + Vehicle), 5) 15 mg/kg PTE-treated APAP group (APAP + PTE15), 6) 30 mg/kg PTE-treated APAP group (APAP + PTE30), 7) 60 mg/kg PTE-treated APAP group (APAP + PTE60), 8) 53 mg/kg RSV-treated APAP group (APAP + RSV53), 9) 60 mg/kg CQ-treated control group (Control + CQ), 10) 60 mg/kg CQ-treated APAP group (APAP + CQ), and 11) 60 mg/kg CQ plus 60 mg/kg PTE-treated APAP group (APAP + PTE60 + CQ). On the basis of serum alanine aminotransferase (ALT) and aspartate aminotransferase (AST) activities, 60 mg/kg PTE was selected as the optimally effective dose for further biochemical studies. Mice were sacrificed at 6 h after APAP treatment. Blood was collected from the inferior vena cava, centrifuged (10,000 rpm, 10 min, 4 °C) to obtain serum, and the serum samples were stored at −75 °C until assayed. Liver tissues were simultaneously isolated and stored at −75 °C until assayed.

2.3. Serum aminotransferase activities

The serum levels of ALT and AST activities were determined by standard spectrophotometric procedures using the Chemilab ALT assay kit and AST assay kit (IVDLab Co., Ltd., Uiwang, Korea), respectively.

2.4. Hematoxylin and eosin (H&E) staining

Liver sections were sampled from a portion of the left lobe and fixed in 10% neutral-buffered formalin, embedded in paraffin, sliced into 5 μm sections, and stained with H&E. Stained sections were examined in randomly chosen histologic fields at 200 × magnification using a light microscope (Olympus CK × 41, Olympus Optical Co., Tokyo, Japan). We utilized the criteria reported by Suzuki et al. (1993) at slightly modification. In this classification, three liver injury indices – sinusoidal congestion (score: 0–4), hepatocyte necrosis (score: 0–4) and ballooning degeneration (score: 0–4) – are graded, for a total score of 0–12. All liver samples have been evaluated by a single pathologist in a blinded fashion.

2.5. Transmission electron microscopy (TEM)

Liver samples were fixed in 2.5% glutaraldehyde and 4% paraformaldehyde in 100 mM sodium phosphate (pH 7.2). Tissues were washed with 100 mM cacodylate (pH 7.4), postfixed in 2% osmium tetroxide, and then washed again. Then, the tissues were dehydrated in a graded series of ethanol and propylene oxide and embedded in epoxy resin (Taab 812 Resin; Canemco Inc., Montreal, QC, Canada). Ultrathin (60–70 nm) sections were counterstained with uranyl acetated and lead citrate, and then viewed using a Hitachi 7600 transmission electron microscope (Hitachi High-Technologies America, Inc., Schaumburg, IL, USA) equipped with a Macrofire monochrome progressive scan CCD camera (Optronics, Inc., Muskogee, OK, USA) and AMTv image capture software (Advanced Microscopy Techniques, Inc., Danvers, MA, USA). In randomly selected fields, we captured 4 non-repeating micrographs for each liver sample (n = 3–4 per group) and the area of one such micrograph was regarded as the unit area. The numbers of autophagic vacuoles per unit area (400 mm^2) in each sample were counted.

2.6. Hepatic lipid peroxidation and glutathione contents

Liver homogenates were analyzed for malondialdehyde (MDA) by measuring the level of thiobarbituric acid-reactive substances spectrophotometrically at 535 nm with 1,1,3,3-tetraethoxypropane (Sigma-Aldrich) as the standard (Buege and Aust, 1978). Total GSH in liver homogenates was determined using yeast-glutathione reductase, 5,5′-

dithiobis(2-nitrobenzoic acid), and nicotinamide adenine dinucleotide phosphate at 412 nm after precipitation with 1% picric acid. Oxidized glutathione (GSSG) levels were determined by the same method in the presence of 2-vinylphyridine, and reduced GSH was calculated as the difference between total GSH and GSSG (Anderson, 1985).

2.7. Western blot analysis

Protein samples were prepared from the microsomal fraction for CYP2E1. Liver tissues were isolated and homogenized in radioimmunoprecipitation assay buffer (150 mM NaCl, 50 mM Tris, 1% Triton X-100, 1% deoxycholic acid, 0.1% sodium dodecyl sulfate, pH 7.4) containing a protease and phosphatase inhibitor mixture for whole protein samples. Protein concentration was determined using a BCA protein assay kit (Pierce Biotechnology Inc, Rockford, IL, USA). Protein samples (16–40 μg) were loaded onto 6–15% sodium dodecyl sulfate-polyacrylamide gels and separated by electrophoresis before being transferred to polyvinylidene fluoride membranes (Millipore, Billerica, MA, USA) using a semidry trans-blot cell (Bio-Rad Laboratories, Hercules, CA, USA). Membranes were blocked for 1 h at room temperature with 5% (w/v) skim milk powder or 5% bovine serum albumin in 0.1% Tween 20 in 1× Tris-buffered saline (TBS/T). Blocked membranes were incubated overnight at 4 °C with primary antibodies. After washing with TBS/T, membranes were incubated with appropriate secondary antibodies for 1 h at room temperature and detected with West-Q Pico ECL Solution (GenDEPOT, Barker, TX, USA). The intensity of the immunoreactive bands was determined using TOTALLAB TL 120 software (Nonlinear Dynamics Ltd., Newcastle, UK). The following primary antibodies were used: CYP2E1 (Gentest, Woburn, MA, USA); autophagy-related protein (Atg)3, Atg7, phosphorylated Unc-51 autophagy activating kinase (ULK1) Ser757, phospho-mammalian target of rapamycin (mTOR), and mTOR (all from Cell Signaling Technology, Beverly, MA, USA); sequestosome-1/p62 (p62) (Abcam, Cambridge, MA, USA), Beclin-1, APG5-APG12 complex (Atg5-Atg12 complex), and cathepsin B (all from Santa Cruz Biotechnology, Santa Cruz, CA, USA); microtubule-associated protein-1 light chain 3 (LC3)-II and lysosome-associated membrane protein (LAMP)-2 (all from Novus Biologicals, Littleton, CO, USA); and β-actin (Sigma-Aldrich). Protein densities were standardized to those of β-actin, and phosphorylated protein densities were standardized to those of total protein for total lysates.

2.8. Statistical analysis

All results are presented as means ± standard error of the mean (SEM). Overall significance of the data was examined by one-way analysis of variance. Differences between groups were considered significant at $p < 0.05$ and $p < 0.01$, with appropriate Bonferroni correction made for multiple comparisons.

3. Results

3.1. Effects of PTE on APAP-induced liver injury

The levels of serum ALT and AST activities in the Control + Vehicle group were 29.3 ± 6.70 U/L and 77.8 ± 7.95 U/L, respectively. At 6 h after APAP treatment, the levels of serum ALT and AST activities significantly increased to 2702.1 ± 212.0 U/L and 1782.1 ± 161.8 U/L, respectively. These increases were attenuated by PTE at 15, 30, and 60 mg/kg in a dose-dependent manner. Moreover, compared with RSV treatment as a positive control, PTE showed more protective potency against hepatotoxicity induced by APAP overdose (Fig. 1A and B). Vehicle (10% Tween 80/Saline) did not affect the serum aminotransferase activities in Control and APAP-treated groups (Data not shown). Based on these results, PTE 60 mg/kg was selected as the optimal effective dose for evaluating the protective mechanisms of PTE in APAP-treated mice. At 24 h after APAP treatment, the levels of serum ALT and AST activities increased to 9587.2 ± 352.7 U/L and 7741.5 ± 612.1 U/L, respectively. PTE treatment showed a tendency to decrease serum ALT (7212.7 ± 700.2 U/L) and AST (6674.1 ± 555.1 U/L) activities (data not shown). Considering the pharmacokinetics of PTE (half-life: 1.73 ± 0.78 h, Remsberg et al., 2008), the additional dosing of PTE could sustain the protective effect against hepatotoxicity at 24 h post-APAP. Morphologic observations of H&E stained specimens demonstrated normal liver architecture in Control + Vehicle and Control + PTE60 groups (Suzuki score: 0.0 ± 0.0 and 0.0 ± 0.0, respectively). In APAP + Vehicle group, the liver sections showed extensive hepatocellular damages, including hepatocyte degeneration and cell death (Suzuki score: 6.3 ± 0.2). PTE60 ameliorated these changes (Suzuki score: 3.8 ± 0.3) (Fig. 1C and D).

3.2. Effects of PTE on oxidative stress in APAP-induced liver injury

Hepatic MDA level in the Control + Vehicle group was 0.38 ± 0.06 nmol/mg protein. APAP administration significantly increased MDA level to 0.57 ± 0.04 nmol/mg protein, and PTE60 attenuated this increase (0.39 ± 0.03 nmol/mg protein) (Fig. 2A). Hepatic GSSG/GSH ratio in the Control + Vehicle group was 0.45 ± 0.09. APAP treatment significantly increased hepatic GSSG/GSH ratio to 2.01 ± 0.02, and this increase was attenuated by PTE60 (1.34 ± 0.11) (Fig. 2B). To confirm the protection by PTE60 is independent of any effect on APAP metabolism, we have measured the GSH contents and CYP2E1 protein expression at early time point (1.5 h after APAP treatment or 30 min post PTE60 treatment). The level of GSH contents was 6.2 ± 0.2 μmol/g liver weight in the Control + Vehicle group. After 1.5 h of APAP treatment (30 min post PTE treatment), the GSH content significantly decreased to 1.4 ± 0.1 μmol/g liver weights. In APAP + PTE60 group, the level of GSH content was 2.1 ± 0.2 μmol/g liver weight, which was not statistically significant compared with the APAP + Vehicle group. Furthermore, there were no differences in the CYP2E1 protein level between APAP + Vehicle and APAP + PTE60 groups (Fig. 2C). These results indicated that PTE protects against APAP-induced hepatotoxicity not through interfering with APAP metabolism.

3.3. Effects of PTE on autophagic flux

The protein expression level of LC3-II, a reliable marker of autophagosomes, significantly increased 2.7-fold compared with that of the control group after APAP treatment. PTE60 enhanced APAP-induced LC3-II protein expression (Fig. 3A). The protein expression level of p62, a selective substrate for autophagy, significantly increased 2.2-fold compared with that of the control group after APAP treatment, and this increase was attenuated by PTE60 (Fig. 3B). Moreover, we utilized the autophagic flux inhibitor CQ to confirm the role of autophagy activation by PTE60 during APAP-induced liver injury. Treatment with CQ abolished the protective effects of PTE60 against APAP-induced liver injury as indicated by increased serum ALT activity and histological changes (Fig. 3C–E). Furthermore, treatment with CQ after PTE60 treatment abolished PTE-induced p62 decrease but did not affect to the increase in LC3-II protein expression (Fig. 3F and G). To confirm our western blot results, we used TEM analysis to observe the autophagic vacuoles. Autophagosomes are characterized by double- and multiple membrane structures containing cytoplasm or undigested organelles including mitochondria. Compared with basal level of autophagic vacuoles in the control group, the number of autophagic vacuoles was markedly increased by APAP treatment and was further increased by PTE60 treatment (Fig. 4A).

3.4. Effects of PTE on autophagosome formation

Initiation of autophagosome formation requires the beclin-1 complex and two conjugation systems: the Atg5-12 conjugation system that

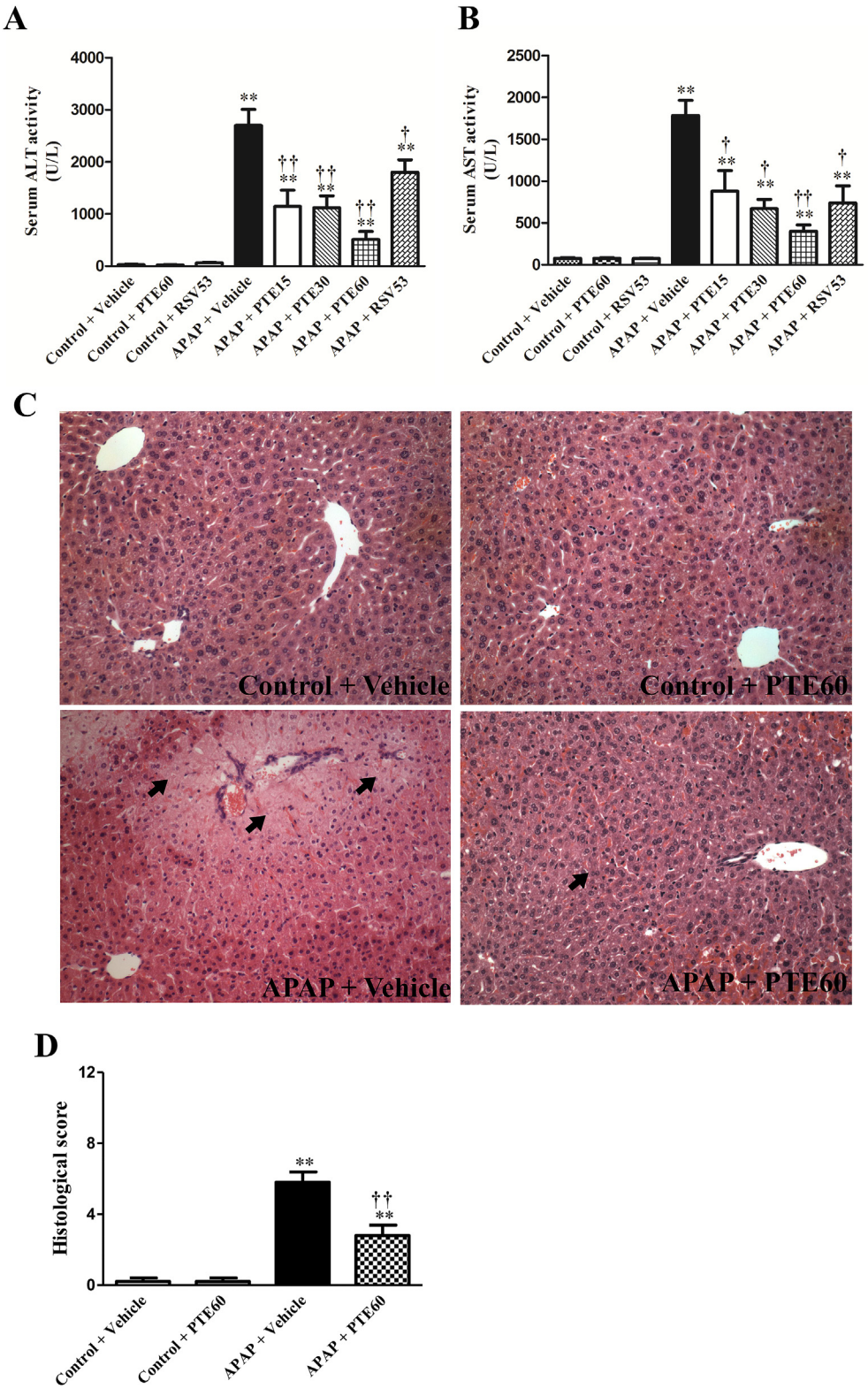

Fig. 1. Effects of PTE on APAP-induced liver injury. Serum levels of (A) ALT and (B) AST activities in male mice treated with various doses of PTE (15, 30 or 60 mg/kg) and RSV 53 mg/kg 1 h after APAP treatment. (C) Representative histological images of liver section stained with H&E at 6 h after APAP treatment. Livers from Control + Vehicle and Control + PTE groups show normal appearance. Liver from APAP + Vehicle groups show hepatocyte degeneration and cell death (closed arrows). PTE attenuates these histological changes. (D) Histological lesions are graded using Suzuki score. Values are presented as means ± SEM (n = 6–8). $^{**}p < 0.01$ compared with the Control + Vehicle group; $^{\dagger}, ^{\dagger\dagger}p < 0.05$, $p < 0.01$ compared with the APAP + Vehicle group.

facilitates binding of LC3-II to the outer membrane of autophagophores and the Atg3 and Atg7 conjugation system that promotes the lipidation of LC3-I to LC3-II. APAP treatment significantly decreased the level of beclin-1 protein expression approximately 65% from that of the control group, and this decrease was attenuated by PTE treatment (Fig. 5A). The Atg5-Atg12 complex protein expression was not affected by APAP treatment, but was increased by PTE treatment (Fig. 5B). Next, we assessed Atg3 and Atg7 protein expression. APAP treatment decreased the levels of Atg3 and Atg7 protein expression approximately 74% and 60%, respectively, from those of the control group. PTE60 attenuated the decreased levels of Atg7 protein expression (Fig. 5C and D).

3.5. Effects of PTE on autophagosome-lysosome fusion and degradation

Once autophagosomes are formed, they fuse with lysosomes to form autolysosomes, and this process is essential to degrade the inner

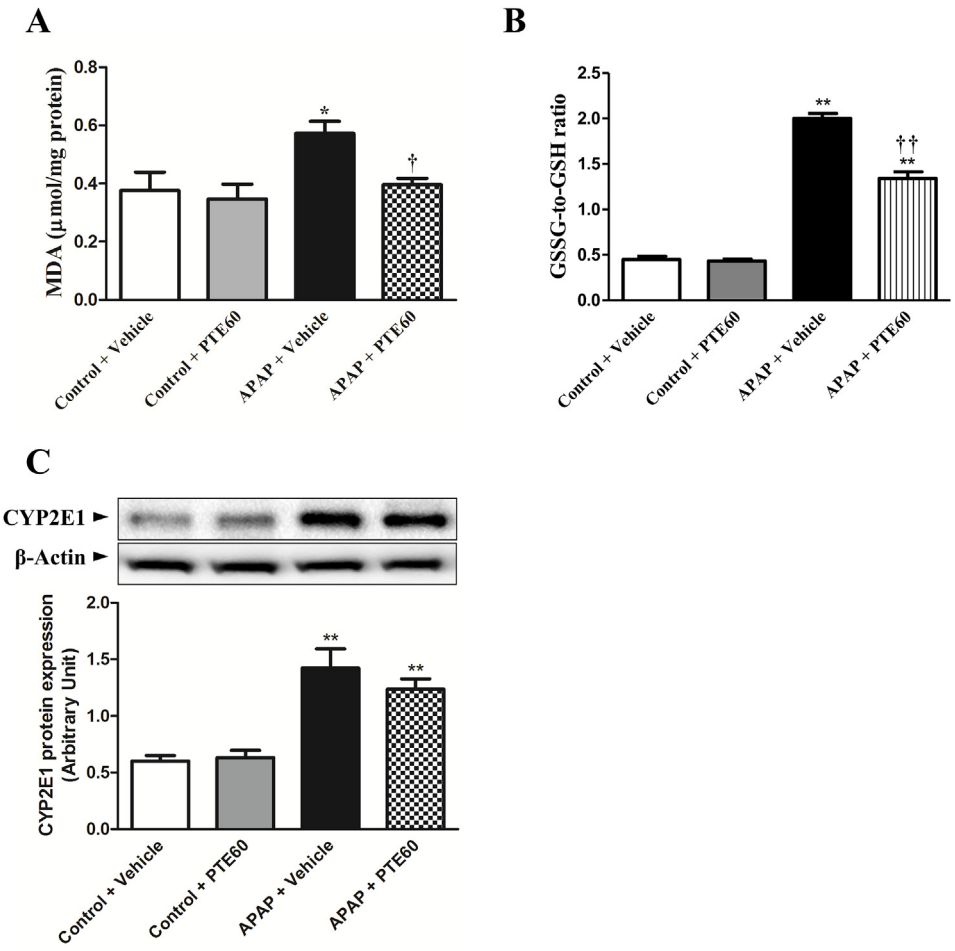

Fig. 2. Effect of PTE on oxidative stress in APAP-induced liver injury. Hepatic levels of (A) MDA and (B) GSSG-to-GSH ratio. Western blot analysis of (C) CYP2E1 protein expression (loading control: β-actin). Values are presented as means ± SEM (n = 6–8). *, $^{**}p < 0.05, p < 0.01$ compared with the Control + Vehicle group; †, $^{\dagger\dagger}p < 0.05, p < 0.01$ compared with the APAP + Vehicle group.

substrates of autophagosomes. We investigated the level of lysosomal membrane protein LAMP-2 protein expression and the lysosomal protease cathepsin B protein expression. As shown in Fig. 6A, the level of LAMP-2 protein expression was significantly decreased in the APAP group to a level approximately 59% from that of the control group, and this decrease was attenuated by PTE treatment. However, there were no significant differences in cathepsin B protein expression among any of the experimental groups (Fig. 6B).

3.6. Effects of PTE on mTOR signaling

To further explore the molecular mechanisms involved in autophagy activation by PTE in APAP-induced liver injury, we investigated the involvement of the mTOR-dependent pathway, a critical regulator of autophagy. Phosphorylation level of mTOR significantly increased 4.1-fold in the APAP-treated group compared to the control group. PTE treatment attenuated this increase (Fig. 7A). Likewise, phosphorylation level of ULK1 Ser757 significantly increased 1.9-fold in APAP-treated group compared to the control group, and PTE60 treatment attenuated this increase (Fig. 7B).

4. Discussion

Autophagy plays a pivotal role in liver diseases; however, the role of autophagy still remains controversial (Rautou et al., 2010). In liver fibrosis, excessive autophagy contributed to liver stellate cell activation and subsequently promoted hepatic fibrogenesis (Hernandez-Gea et al., 2013). APAP overdose induced autophagy, which eliminated damaged mitochondria and attenuated hepatocyte necrosis (Ni et al., 2012). In contrast, acute alcohol consumption impaired autophagy, which leads to apoptotic cell death in mouse liver (Yang et al., 2014). A plethora of evidence had demonstrated that ROS can activate starvation-induced autophagy and autophagic cell death (Huang et al., 2011). PTE, a dimethyl analogue of RSV, had potent antioxidant and anti-inflammatory properties (McCormack and McFadden, 2012). PTE ameliorated APAP-induced liver injury by increasing antioxidant activity and inhibiting inflammatory cytokine release (El-Sayed el et al., 2015). Cheng et al. (2014) showed that PTE had anti-cancer activity through induction of autophagy in a COLO 205 colon cancer cell line. In the present study, we investigated the molecular mechanism by which PTE protects against APAP-induced liver injury, with a focus on autophagic flux in mice.

Autophagy is an intracellular process consists of complex molecular machinery in which cytoplasmic proteins or organelles are sequestered by autophagosomes and delivered to lysosomes for proteolytic degradation. Earlier studies indicated that activation of autophagy serves a cellular adaptive mechanism to counteract APAP-induced hepatotoxicity, based on the finding of increased LC3-II accumulation (Ni et al., 2012; Igusa et al., 2012). LC3-II is known to only present on mature autophagosomes and is regarded as a typical indicator of autophagic flux, however, it is ambiguous whether increased LC3-II protein expression can be translated as an induction of autophagy or impairment of autophagy by blockage of lysosomal fusion and degradation (Kuma et al., 2007). For example, LC3-II expression was

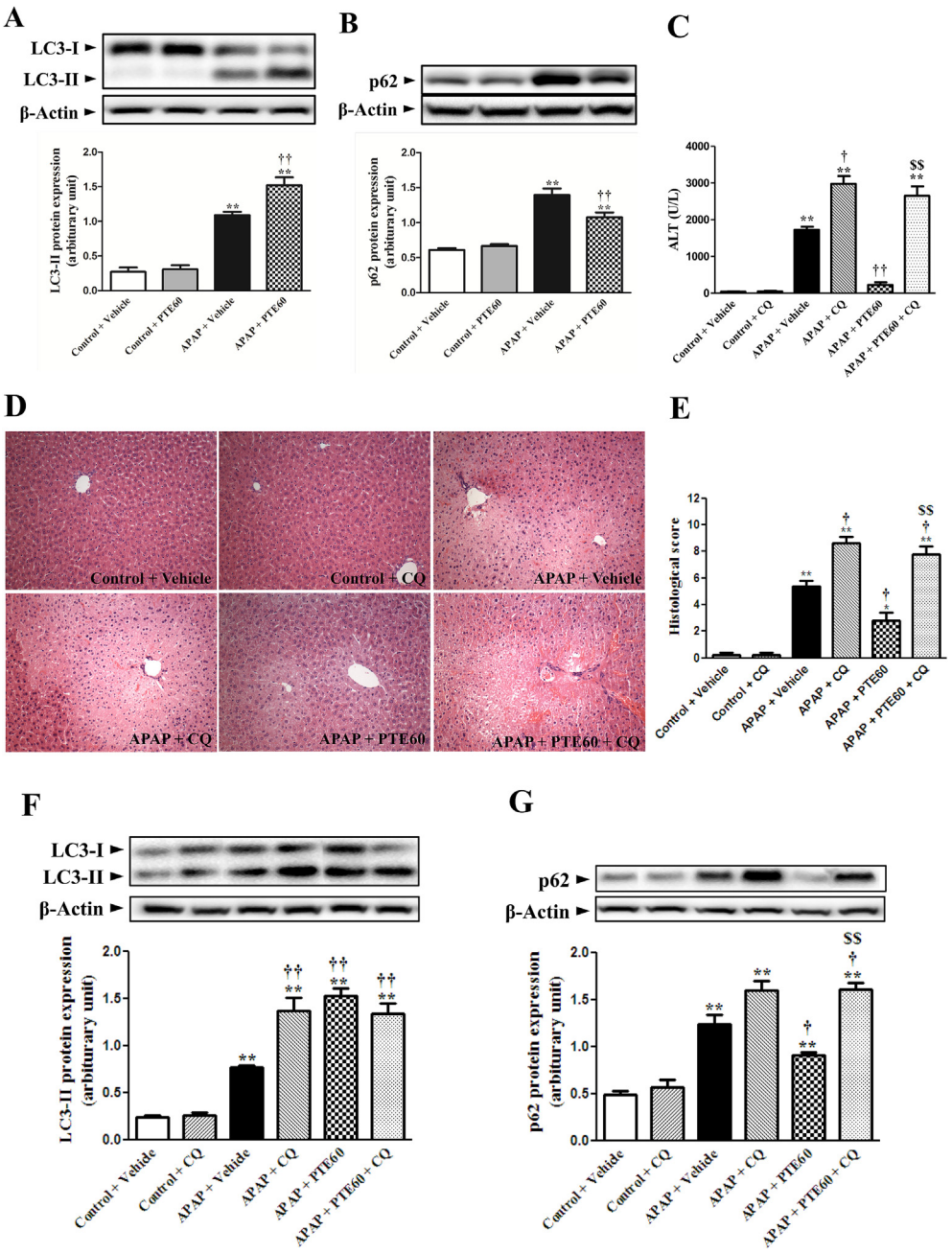

Fig. 3. Effect of PTE on autophagic flux. Western blot analysis of hepatic (A) LC3-II and (B) p62 protein expressions (loading control: β-actin). Effect of CQ in the presence of PTE on (C) serum ALT activity and (D) representative histological images of liver section stained with H&E at 6 h after APAP treatment. (E) Histological lesions are graded using Suzuki score. Effect of CQ in the presence of PTE on western blot analysis of (F) hepatic LC3-II, (G) p62 protein expressions (loading control: β-actin) and Values are presented as means ± SEM (n = 6–8). *, $^{**}p < 0.05$, $p < 0.01$ compared with the Control + Vehicle group; †, $^{\dagger\dagger}p < 0.05$, $p < 0.01$ compared with the APAP + Vehicle group; $^{\$\$}p < 0.01$ compared with the APAP + PTE60 group.

found to be significantly increased in a non-alcoholic fatty liver disease model of mice; however, this was not the result of autophagy induction but rather impairment of autolysosome function (Gonzalez-Rodriguez et al., 2014). The autophagic substrate p62, normally degraded during autophagy, is an ubiquitin binding protein that recognizes ubiquitinated substrates and recruits phagophores through direct interaction with LC3-II (Lamark et al., 2003; Pankiv et al., 2007). Since LC3-II and p62 are both degraded in the autolysosome with autophagic cargo, accumulation of LC3-II and p62 is regarded as a robust marker of impaired autophagic flux (Lee et al., 2012). Previous study demonstrated that expression of p62 gene is induced by Nrf2 upon exposure to ROS (Jain et al., 2010). Nrf2 regulates the antioxidant response by activating a battery of genes bearing an antioxidant response element (ARE). In our study, APAP overdose did not affect mRNA expression of p62 (data not shown), suggesting that p62 turnover comes from autophagic degradation as its substrates. LC3-II and p62 protein expression significantly increased after APAP treatment. Treatment with CQ, an inhibitor of lysosomal acidification did not affect APAP-induced increase of LC3-II, further accumulated p62 and exacerbated liver injury, as evidenced by increased levels of serum ALT activity and histological damages. These results indicate that impaired autophagic flux is responsible for APAP-induced liver injury. However, other studies have demonstrated that APAP overdose treatment increased LC3-II and degraded p62, indicating that activated autophagy protects against APAP through clearance of damaged mitochondria and detrimental APAP adducts formation (Ni et al., 2012, 2016). Recently, Wang et al. (2016) reported that higher concentration of APAP (> 15 mM) markedly inhibited LC3-II level in hepatocytes, whereas LC3-II levels were increased by 2.5 mM or 5 mM APAP. The level of p62 and phosphor-p62 were significantly increased at 6 h following administration of APAP and reached their peaks at 12 h (Shen et al., 2018). The discrepancies between our results with others might be derived from different experimental settings (e.g. *in vivo vs in vitro*, different mice strain, dosing and timing of APAP). PTE increased LC3-II expression and reduced p62

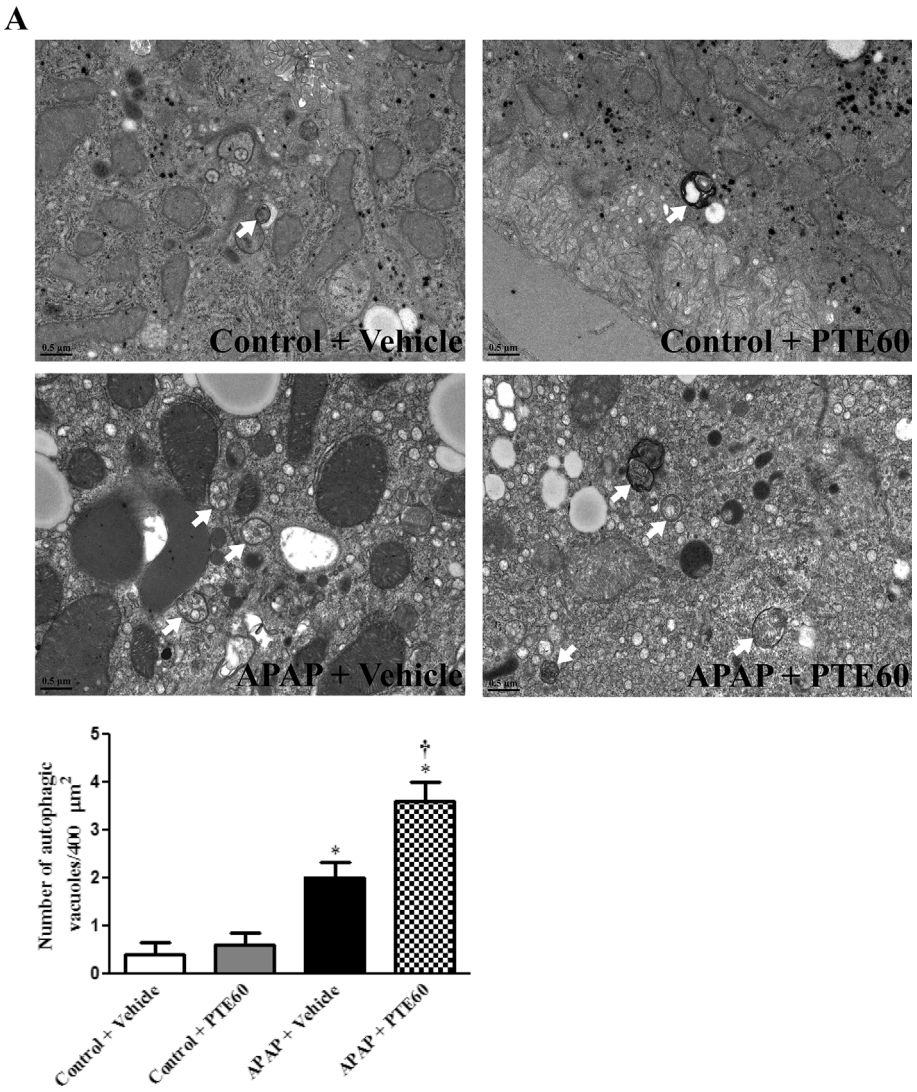

Fig. 4. Representative TEM images of autophagic vacuoles from liver tissue. Autophagic vacuoles are indicated closed arrows. (A) Livers from Control + Vehicle and Control + PTE60 groups shows few autophagic vacuoles. Liver from APAP + Vehicle group shows increased autophagic vacuoles and PTE60 enhanced more autophagic vacuoles. $^{*}p < 0.05$ compared with the Control + Vehicle group; $^{\dagger}p < 0.05$ compared with the APAP + Vehicle group.

accumulation, thereby attenuating liver injury due to decreased serum ALT and AST activities. TEM images revealed that PTE further increased the number of autophagic vacuoles in the livers of mice during APAP overdose, which correlated with our western blot results. To confirm autophagy activation by PTE and its possible contribution to attenuation of liver damage triggered by APAP, we utilized CQ. Co-treatment with CQ blocked the restoration of autophagic flux by PTE and diminished the hepatoprotective effects of PTE on APAP overdose. Collectively, our data suggest that PTE alleviates APAP-induced liver injury by restoring the impaired autophagic flux.

Precise interaction between the autophagy machinery and autophagy receptors are critical for execution of an integrated autophagy process. The process of autophagy consists of several sequential key steps: membrane isolation, phagophore elongation, autophagosome formation, and autophagosome-lysosome fusion and degradation. After the Beclin-1 complex initiates membrane isolation and recruits autophagic proteins required for autophagosome formation, two conjugation systems play crucial roles in the formation of autophagosome: the Atg5-Atg12 conjugation system and LC3 lipidation system. The Atg5-Atg12 conjugation system is present on the outer side of the isolated membrane and LC3-II subsequently binds to the Atg5-Atg12-associated phagophore to form a mature autophagosome. Pre-LC3 is cleaved by Atg4 to LC3-I, which covalently binds to phosphatidyl ethanolamine by the action of Atg7 and Atg3 proteins and finally becomes LC3-II. Total saponins enhanced autophagy via up-regulation of Beclin-1 and Atg5 protein expression which prevented APAP-induced liver damage (Dong et al., 2014). Igusa et al. (2012) reported that genetic deletion of Atg7 impaired autophagy, which accelerated necrotic and apoptotic cell death of hepatocytes induced by APAP overdose. In the present study, APAP overdose significantly decreased Beclin-1, Atg3, and Atg7 protein expression. PTE increased Beclin-1 and Atg7 protein expression as well as Atg5-Atg12 conjugate protein expression indicating that PTE induces phagophore elongation and increases mature autophagosome formation.

Last stage of autophagy is a fusion of lysosomes with mature autophagosomes, which is a crucial step for degradation of autophagic cargo (Yu et al., 2010). LAMP-2 is especially important for termination of autophagy, as a main membrane protein of autophagosome and lysosome fusion (Eskelinen et al., 2002). A combination of alcohol and lipopolysaccharides inhibited the autophagosome and lysosome fusion via down-regulation of LAMP-2 protein expression, which enhanced pancreatic acinar cell necrosis (Fortunato et al., 2009). Cathepsin, a representative member of the lysosomal proteases, has also been shown to play a key role in autolysosome degradation (Uchiyama, 2001).

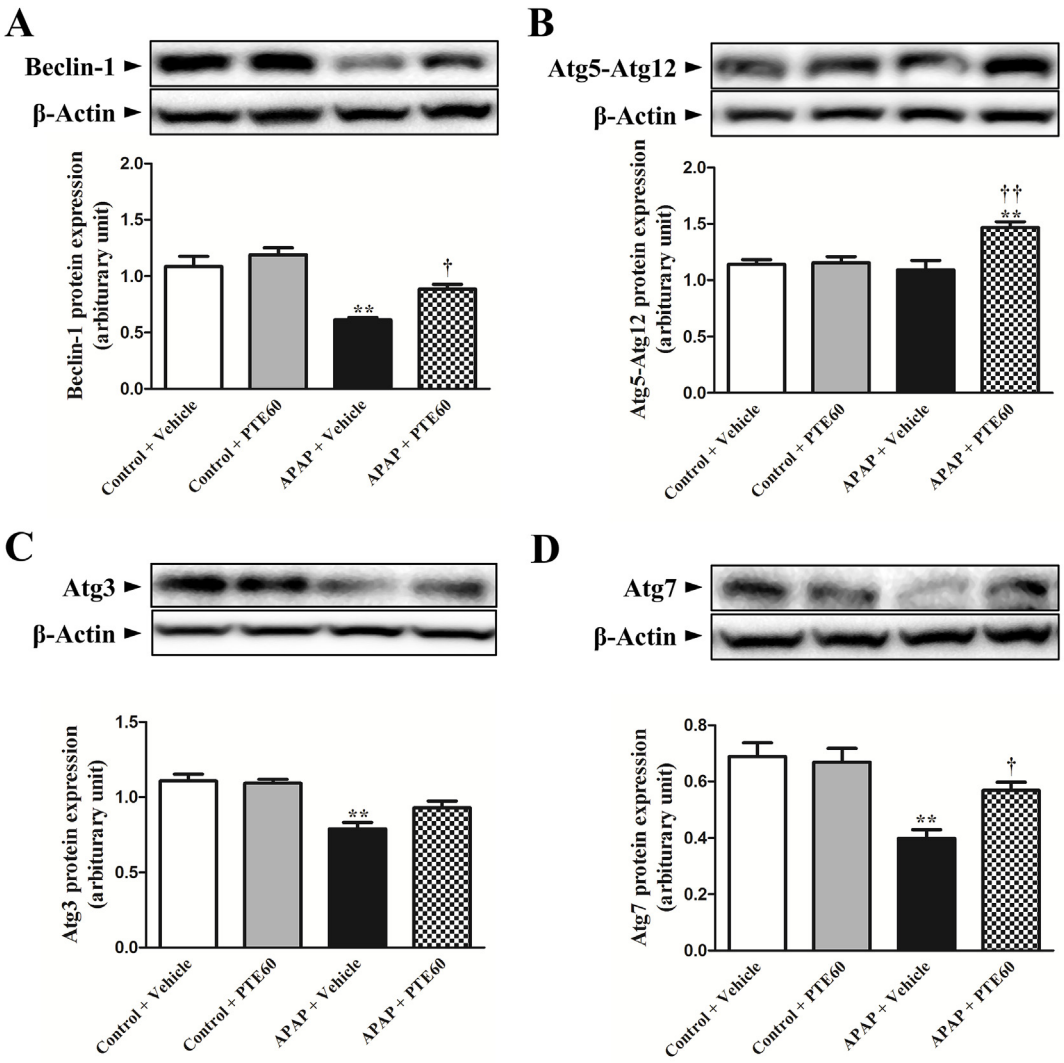

Fig. 5. Effect of PTE on autophagosome formation. Western blot analysis of hepatic (A) beclin-1, (B) Atg5-Atg12 protein complex, (C) Atg3 and (D) Atg7 protein expressions (loading control: β-actin). Values are presented as means ± SEM (n = 6–8). $^{**}p < 0.01$ compared with the Control + Vehicle group; $^{\dagger, \dagger\dagger}p < 0.05$, $p < 0.01$ compared with the APAP + Vehicle group.

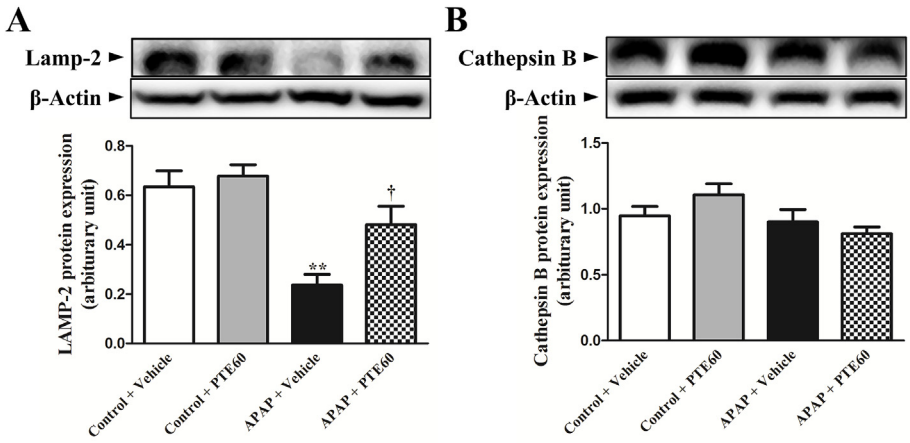

Fig. 6. Effect of PTE on autophagosome-lysosome fusion and degradation. Western blot analysis of hepatic (A) LAMP-2 and (B) cathepsin B protein expressions (loading control: β-actin). Values are presented as means ± SEM (n = 6–8). $^{**}p < 0.01$ compared with the Control + Vehicle group; $^{\dagger}p < 0.05$ compared with the APAP + Vehicle group.

Defective cathepsin B and cathepsin L enzyme activity resulted in insufficient autolysosome clearance and accumulation of autophagic vacuoles, which contributed to the initiation of pancreatitis (Mareninova et al., 2009). However, another study found that z-FA-FMK, a cathepsin B inhibitor, did not significantly affect APAP-induced liver injury in of mice (Woolbright et al., 2012). In our study, APAP overdose significantly decreased LAMP-2 protein expression, but not cathepsin B protein expression. PTE increased the LAMP-2 protein expression.

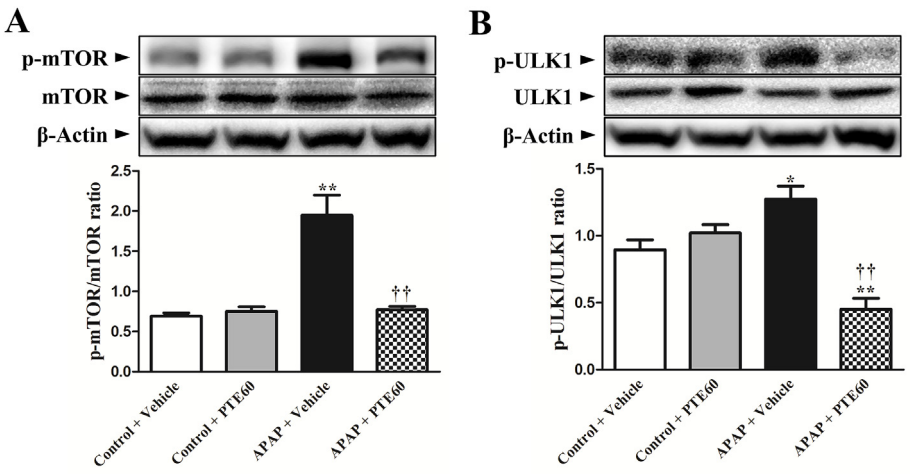

Fig. 7. Effect of PTE on mTOR signaling. Western blot analysis of hepatic (A) mTOR and (B) ULK1 Ser757 protein phosphorylation (loading control: β-actin). Values are presented as means ± SEM (n = 6–8). $^{*}, ^{**}p < 0.05, p < 0.01$ compared with the Control + Vehicle group; $^{\dagger\dagger}p < 0.01$ compared with the APAP + Vehicle group.

These results suggest that PTE restores autophagosome-lysosome fusion.

mTOR, a serine/threonine protein kinase, is a major intracellular hub for integrating autophagy-related signals (Jung et al., 2010) which regulates diverse cellular processes and is the main upstream negative effector of autophagy in mammalian cells (Wullschleger et al., 2006). ULK1, a mammalian homolog of Atg1, is localized in the isolated membrane and recruits the Beclin-1 complex (Nazio et al., 2013). mTOR inhibits ULK1 activation by phosphorylating ULK1 Ser757 and disrupting its interaction with AMP activated protein kinase (Kim et al., 2011). Acute alcohol consumption activates mTOR signaling and decreases Beclin-1 and Atg7 protein expressions, which results in liver steatosis (Yang et al., 2012). Rapamycin induces LC3-II protein expression through inhibition of mTOR signaling and subsequently protects the liver from I/R injury (Zhu et al., 2015). In the present study, APAP overdose significantly increased phosphorylation levels of mTOR and ULK1 Ser757, while PTE attenuated these increases. Overall, our data suggest that PTE suppresses mTOR signaling.

In conclusion, our findings suggest that PTE protects against APAP-induced liver injury by restoring impaired autophagic flux. Our study demonstrates the influence of PTE on the autophagy machinery in APAP overdosed liver, focusing on the sequential steps of autophagy. Therefore, we propose that PTE may provide a new pharmacological maneuver for drug-induced acute liver failure.

Conflicts of interest

The authors declare no conflicts of interest.

Acknowledgements

This research was supported by the Mid-Career Researcher Program through an NRF grant funded by the Ministry of Education, Science and Technology in Korea (NRF-2016R1A2B4009880).

Transparency document

Transparency document related to this article can be found online at https://doi.org/10.1016/j.fct.2018.12.012

References

Amar, P.J., Schiff, E.R., 2007. Acetaminophen safety and hepatotoxicity—where do we go from here? Expert Opin. Drug Saf. 6, 341–355.

Anderson, M.E., 1985. Determination of glutathione and glutathione disulfide in biological samples. Methods Enzymol. 113, 548–555.

Bhakkiyalakshmi, E., Sireesh, D., Sakthivadivel, M., Sivasubramanian, S., Gunasekaran, P., Ramkumar, K.M., 2016. Anti-hyperlipidemic and anti-peroxidative role of pterostilbene via Nrf2 signaling in experimental diabetes. Eur. J. Pharmacol. 777, 9–16.

Buege, J.A., Aust, S.D., 1978. Microsomal lipid peroxidation. Methods Enzymol. 52, 302–310.

Cheng, T.C., Lai, C.S., Chung, M.C., Kalyanam, N., Majeed, M., Ho, C.T., Ho, Y.S., Pan, M.H., 2014. Potent anti-cancer effect of 3'-hydroxypterostilbene in human colon xenograft tumors. PLoS One 9, e111814.

Cho, H.I., Kim, S.J., Choi, J.W., Lee, S.M., 2016. Genipin alleviates sepsis-induced liver injury by restoring autophagy. Br. J. Pharmacol. 173, 980–991.

Dong, D., Xu, L., Han, X., Qi, Y., Xu, Y., Yin, L., Liu, K., Peng, J., 2014. Effects of the total saponins from Rosa laevigata Michx fruit against acetaminophen-induced liver damage in mice via induction of autophagy and suppression of inflammation and apoptosis. Molecules 19, 7189–7206.

du Toit, A., Hofmeyr, J.S., Gniadek, T.J., Loos, B., 2018. Measuring autophagosome flux. Autophagy 14, 1060–1071.

El-Sayed el, S.M., Mansour, A.M., Nady, M.E., 2015. Protective effects of pterostilbene against acetaminophen-induced hepatotoxicity in rats. J. Biochem. Mol. Toxicol. 29, 35–42.

Eskelinen, E.L., Illert, A.L., Tanaka, Y., Schwarzmann, G., Blanz, J., Von Figura, K., Saftig, P., 2002. Role of LAMP-2 in lysosome biogenesis and autophagy. Mol. Biol. Cell 13, 3355–3368.

Fortunato, F., Burgers, H., Bergmann, F., Rieger, P., Buchler, M.W., Kroemer, G., Werner, J., 2009. Impaired autolysosome formation correlates with Lamp-2 depletion: role of apoptosis, autophagy, and necrosis in pancreatitis. Gastroenterology 137, 350–360 360.e351-355.

Gonzalez-Rodriguez, A., Mayoral, R., Agra, N., Valdecantos, M.P., Pardo, V., Miquilena-Colina, M.E., Vargas-Castrillon, J., Lo Iacono, O., Corazzari, M., Fimia, G.M., Piacentini, M., Muntane, J., Bosca, L., Garcia-Monzon, C., Martin-Sanz, P., Valverde, A.M., 2014. Impaired autophagic flux is associated with increased endoplasmic reticulum stress during the development of NAFLD. Cell Death. Dis. 5, e1179.

Hernandez-Gea, V., Hilscher, M., Rozenfeld, R., Lim, M.P., Nieto, N., Werner, S., Devi, L.A., Friedman, S.L., 2013. Endoplasmic reticulum stress induces fibrogenic activity in hepatic stellate cells through autophagy. J. Hepatol. 59, 98–104.

Hougee, S., Faber, J., Sanders, A., de Jong, R.B., van den Berg, W.B., Garssen, J., Hoijer, M.A., Smit, H.F., 2005. Selective COX-2 inhibition by a pterocarpus marsupium extract characterized by pterostilbene, and its activity in healthy human volunteers. Planta Med. 71, 387–392.

Huang, J., Lam, G.Y., Brumeil, J.H., 2011. Autophagy signaling through reactive oxygen species. Antioxidants Redox Signal. 14, 2215–2231.

Igusa, Y., Yamashina, S., Izumi, K., Inami, Y., Fukada, H., Komatsu, M., Tanaka, K., Ikejima, K., Watanabe, S., 2012. Loss of autophagy promotes murine acetaminophen hepatotoxicity. J. Gastroenterol. 47, 433–443.

Jaeschke, H., McGill, M.R., Ramachandran, A., 2012. Oxidant stress, mitochondria, and cell death mechanisms in drug-induced liver injury: lessons learned from acetaminophen hepatotoxicity. Drug Metab. Rev. 44, 88–106.

Jaeschke, H., McGill, M.R., Williams, C.D., Ramachandran, A., 2011. Current issues with acetaminophen hepatotoxicity–a clinically relevant model to test the efficacy of natural products. Life Sci. 88, 737–745.

Jain, A., Lamark, T., Sjøttem, E., Larsen, K.B., Awuh, J.A., Øvervatn, A., McMahon, M., Hayes, J.D., Johansen, T., 2010. p62/SQSTM1 is a target gene for transcription factor NRF2 and creates a positive feedback loop by inducing antioxidant response element-driven gene transcription. J. Biol. Chem. 285, 22576–22591.

James, L.P., Mayeux, P.R., Hinson, J.A., 2003. Acetaminophen-induced hepatotoxicity. Drug Metab. Dispos. 31, 1499–1506.

Jung, C.H., Ro, S.H., Cao, J., Otto, N.M., Kim, D.H., 2010. mTOR regulation of autophagy. FEBS Lett. 584, 1287–1295.
Kapetanovic, I.M., Muzzio, M., Huang, Z., Thompson, T.N., McCormick, D.L., 2011. Pharmacokinetics, oral bioavailability, and metabolic profile of resveratrol and its dimethylether analog, pterostilbene, in rats. Cancer Chemother. Pharmacol. 68, 593–601.
Kim, J., Kundu, M., Viollet, B., Guan, K.L., 2011. AMPK and mTOR regulate autophagy through direct phosphorylation of Ulk1. Nat. Cell Biol. 13, 132–141.
Ko, C.P., Lin, C.W., Chen, M.K., Yang, S.F., Chiou, H.L., Hsieh, M.J., 2015. Pterostilbene induce autophagy on human oral cancer cells through modulation of Akt and mitogen-activated protein kinase pathway. Oral Oncol. 51, 593–601.
Kuma, A., Matsui, M., Mizushima, N., 2007. LC3, an autophagosome marker, can be incorporated into protein aggregates independent of autophagy: caution in the interpretation of LC3 localization. Autophagy 3, 323–328.
Lamark, T., Perander, M., Outzen, H., Kristiansen, K., Overvatn, A., Michaelsen, E., Bjorkoy, G., Johansen, T., 2003. Interaction codes within the family of mammalian Phox and Bem1p domain-containing proteins. J. Biol. Chem. 278, 34568–34581.
Larson, A.M., 2007. Acetaminophen hepatotoxicity. Clin. Liver Dis. 11, 525–548.
Lee, H.S., Daniels, B.H., Salas, E., Bollen, A.W., Debnath, J., Margeta, M., 2012. Clinical utility of LC3 and p62 immunohistochemistry in diagnosis of drug-induced autophagic vacuolar myopathies: a case-control study. PLoS One 7, e36221.
Lee, M.F., Liu, M.L., Cheng, A.C., Tsai, M.L., Ho, C.T., Liou, W.S., Pan, M.H., 2013. Pterostilbene inhibits dimethylnitrosamine-induced liver fibrosis in rats. Food Chem. 138, 802–807.
Lee, S.M., Cho, T.S., Kim, D.J., Cha, Y.N., 1999. Protective effect of ethanol against acetaminophen-induced hepatotoxicity in mice: role of NADH:quinone reductase. Biochem. Pharmacol. 58, 1547–1555.
Lee, W.M., Hynan, L.S., Rossaro, L., Fontana, R.J., Stravitz, R.T., Larson, A.M., Davern 2nd, T.J., Murray, N.G., McCashland, T., Reisch, J.S., Robuck, P.R., 2009. Intravenous N-acetylcysteine improves transplant-free survival in early stage non-acetaminophen acute liver failure. Gastroenterology 137, 856–864 864.e851.
Lin, C.W., Chou, Y.E., Chiou, H.L., Chen, M.K., Yang, W.E., Hsieh, M.J., Yang, S.F., 2014a. Pterostilbene suppresses oral cancer cell invasion by inhibiting MMP-2 expression. Expert Opin. Ther. Targets 18, 1109–1120.
Lin, Z., Wu, F., Lin, S., Pan, X., Jin, L., Lu, T., Shi, L., Wang, Y., Xu, A., Li, X., 2014b. Adiponectin protects against acetaminophen-induced mitochondrial dysfunction and acute liver injury by promoting autophagy in mice. J. Hepatol. 61, 825–831.
Lv, M., Liu, K., Fu, S., Li, Z., Yu, X., 2015. Pterostilbene attenuates the inflammatory reaction induced by ischemia/reperfusion in rat heart. Mol. Med. Rep. 11, 724–728.
Mahmoudi, G.A., Astaraki, P., Mohtashami, A.Z., Ahadi, M., 2015. N-acetylcysteine overdose after acetaminophen poisoning. Int. Med. Case Rep. J. 8, 65–69.
Mareninova, O.A., Hermann, K., French, S.W., O'Konski, M.S., Pandol, S.J., Webster, P., Erickson, A.H., Katunuma, N., Gorelick, F.S., Gukovsky, I., Gukovskaya, A.S., 2009. Impaired autophagic flux mediates acinar cell vacuole formation and trypsinogen activation in rodent models of acute pancreatitis. J. Clin. Invest. 119, 3340–3355.
McCormack, D., McFadden, D., 2012. Pterostilbene and cancer: current review. J. Surg. Res. 173, e53–61.
Muriel, P., Garciapiña, T., Perez-Alvarez, V., Mourelle, M., 1992. Silymarin protects against paracetamol-induced lipid peroxidation and liver damage. J. Appl. Toxicol. 12, 439–442.
Nazio, F., Strappazzon, F., Antonioli, M., Bielli, P., Cianfanelli, V., Bordi, M., Gretzmeier, C., Dengjel, J., Piacentini, M., Fimia, G.M., Cecconi, F., 2013. mTOR inhibits autophagy by controlling ULK1 ubiquitylation, self-association and function through AMBRA1 and TRAF6. Nat. Cell Biol. 15, 406–416.
Ni, H.M., Bockus, A., Boggess, N., Jaeschke, H., Ding, W.X., 2012. Activation of autophagy protects against acetaminophen-induced hepatotoxicity. Hepatology 55, 222–232.
Ni, H.M., McGill, M.R., Chao, X., Du, K., Williams, J.A., Xie, Y., Jaeschke, H., Ding, W.X., 2016. Removal of acetaminophen protein adducts by autophagy protects against acetaminophen-induced liver injury in mice. J. Hepatol. 65, 354–362.
Pankiv, S., Clausen, T.H., Lamark, T., Brech, A., Bruun, J.A., Outzen, H., Overvatn, A., Bjorkoy, G., Johansen, T., 2007. p62/SQSTM1 binds directly to Atg8/LC3 to facilitate degradation of ubiquitinated protein aggregates by autophagy. J. Biol. Chem. 282, 24131–24145.
Park, J.H., Seo, K.S., Tadi, S., Ahn, B.H., Lee, J.U., Heo, J.Y., Han, J., Song, M.S., Kim, S.H., Yim, Y.H., Choi, H.S., Shong, M., Kweon, G., 2013. An indole derivative protects against acetaminophen-induced liver injury by directly binding to N-acetyl-p-benzoquinone imine in mice. Antioxidants Redox Signal. 18, 1713–1722.
Rautou, P.E., Mansouri, A., Lebrec, D., Durand, F., Valla, D., Moreau, R., 2010. Autophagy in liver diseases. J. Hepatol. 53, 1123–1134.
Remsberg, C.M., Yáñez, J.A., Ohgami, Y., Vega-Villa, K.R., Rimando, A.M., Davies, N.M., 2008. Pharmacometrics of pterostilbene: preclinical pharmacokinetics and metabolism, anticancer, antiinflammatory, antioxidant and analgesic activity. Phytother. Res. 22, 169–179.
Rimando, A.M., Cuendet, M., Desmarchelier, C., Mehta, R.G., Pezzuto, J.M., Duke, S.O., 2002. Cancer chemopreventive and antioxidant activities of pterostilbene, a naturally occurring analogue of resveratrol. J. Agric. Food. Chem. 50, 3453–3457.
Sener, G., Toklu, H.Z., Sehirli, A.O., Velioğlu-Oğünç, A., Cetinel, S., Gedik, N., 2006. Protective effects of resveratrol against acetaminophen-induced toxicity in mice. Hepatol. Res. 35, 62–68.
Shen, Z., Wang, Y., Su, Z., Kou, R., Xie, K., Song, F., 2018. Activation of p62-keap1-Nrf2 antioxidant pathway in the early stage of acetaminophen-induced acute liver injury in mice. Chem. Biol. Interact. 282, 22–28.
Somanawat, K., Thong-Ngam, D., Klaikeaw, N., 2013. Curcumin attenuated paracetamol overdose induced hepatitis. World J. Gastroenterol. 19, 1962–1967.
Suzuki, S., Toledo-Pereyra, L.H., Rodriguez, F.J., Cejalvo, D., 1993. Neutrophil infiltration as an important factor in liver ischemia and reperfusion injury. Modulating effects of FK506 and cyclosporine. Transplantation 55, 1265–1272.
Szajdek, A., Borowska, E.J., 2008. Bioactive compounds and health-promoting properties of berry fruits: a review. Plant Foods Hum. Nutr. 63, 147–156.
Uchiyama, Y., 2001. Autophagic cell death and its execution by lysosomal cathepsins. Arch. Histol. Cytol. 64, 233–246.
Wang, Q., Guo, W., Hao, B., Shi, X., Lu, Y., Wong, C.W., Ma, V.W., Yip, T.T., Au, J.S., Hao, Q., Cheung, K.H., Wu, W., Li, G.R., Yue, J., 2016. Mechanistic study of TRPM2-Ca (2+)-CAMK2-BECN1 signaling in oxidative stress-induced autophagy inhibition. Autophagy 12, 1340–1354.
Woolbright, B.L., Ramachandran, A., McGill, M.R., Yan, H.M., Bajt, M.L., Sharpe, M.R., Lemasters, J.J., Jaeschke, H., 2012. Lysosomal instability and cathepsin B release during acetaminophen hepatotoxicity. Basic Clin. Pharmacol. Toxicol. 111, 417–425.
Wu, X., He, L., Chen, F., He, X., Cai, Y., Zhang, G., Yi, Q., He, M., Luo, J., 2014. Impaired autophagy contributes to adverse cardiac remodeling in acute myocardial infarction. PLoS One 9, e112891.
Wullschleger, S., Loewith, R., Hall, M.N., 2006. TOR signaling in growth and metabolism. Cell 124, 471–484.
Yang, L., Rozenfeld, R., Wu, D., Devi, L.A., Zhang, Z., Cederbaum, A., 2014. Cannabidiol protects liver from binge alcohol-induced steatosis by mechanisms including inhibition of oxidative stress and increase in autophagy. Free Radic. Biol. Med. 68, 260–267.
Yang, L., Wu, D., Wang, X., Cederbaum, A.I., 2012. Cytochrome P4502E1, oxidative stress, JNK, and autophagy in acute alcohol-induced fatty liver. Free Radic. Biol. Med. 53, 1170–1180.
Yu, L., McPhee, C.K., Zheng, L., Mardones, G.A., Rong, Y., Peng, J., Mi, N., Zhao, Y., Liu, Z., Wan, F., Hailey, D.W., Oorschot, V., Klumperman, J., Baehrecke, E.H., Lenardo, M.J., 2010. Termination of autophagy and reformation of lysosomes regulated by mTOR. Nature 465, 942–946.
Zai, W., Chen, W., Luan, J., Fan, J., Zhang, X., Wu, Z., Ding, T., Ju, D., Liu, H., 2018. Dihydroquercetin ameliorated acetaminophen-induced hepatic cytotoxicity via activating JAK2/STAT3 pathway and autophagy. Appl. Microbiol. Biotechnol. 102, 1443–1453.
Zhang, L., Cui, L., Zhou, G., Jing, H., Guo, Y., Sun, W., 2013. Pterostilbene, a natural small-molecular compound, promotes cytoprotective macroautophagy in vascular endothelial cells. J. Nutr. Biochem. 24, 903–911.
Zhu, J., Lu, T., Yue, S., Shen, X., Gao, F., Busuttil, R.W., Kupiec-Weglinski, J.W., Xia, Q., Zhai, Y., 2015. Rapamycin protection of livers from ischemia and reperfusion injury is dependent on both autophagy induction and mammalian target of rapamycin complex 2-Akt activation. Transplantation 99, 48–55.